Strangulation in a high redshift cluster revealed by enhanced metallicities and ALMA molecular gas

Based mainly on

Maier, Hayashi, Ziegler & Kodama,

2019b, A&A, 626, A14

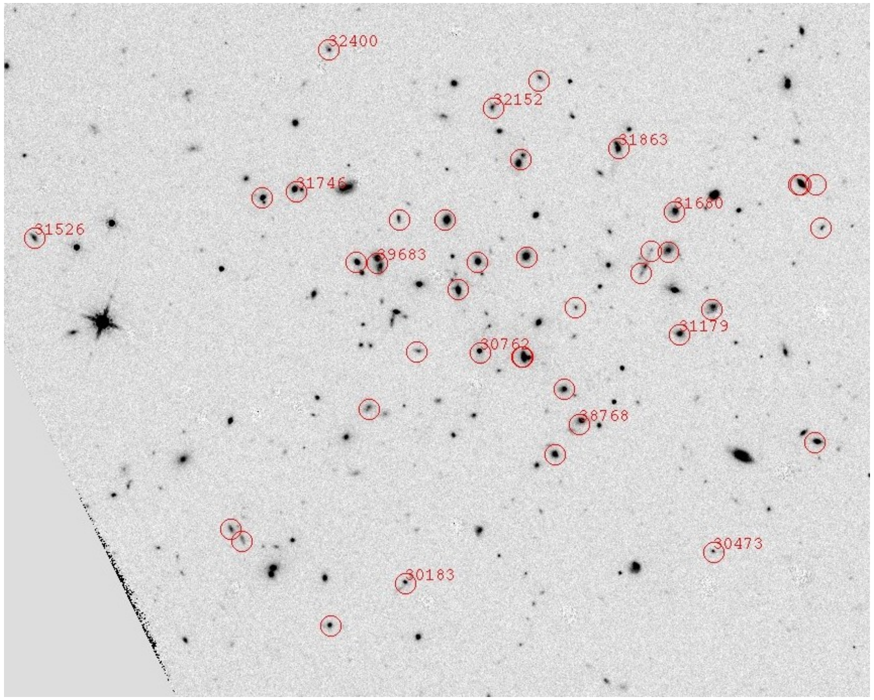

universität wien

Christian Maier

Institut für Astrophysik

Slow quenching: strangulation/starvation/suffocation

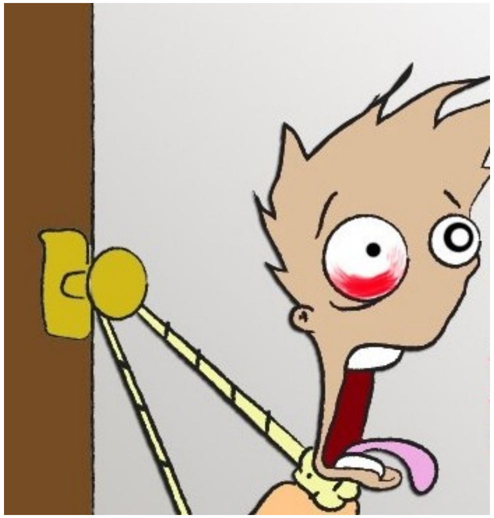

In humans: death by strangulation is a slow process

- victim uses up oxygen in the lungs but keeps producing carbon dioxide, which remains trapped in the body
- high levels of carbon dioxide in the blood of a corpse suggest strangulation/suffocation

In galaxies: strangulation is a slow star formation quenching process (e.g., Peng et al. 2015, Maier et al. 2016, 2019a,b)

- the supply of pristine gas (which would otherwise dillute the ISM) onto the galaxy disk is halted, but star formation can continue, using the gas available in the disk until it is completely used up
- instead of building carbon dioxide (cf. humans), the strangled galaxies accumulate metals produced by massive stars (no gas dillution of their ISM by pristine gas inflow)
- higher gas metallicities: evidence for galactic “strangulation” or “suffocation”

Lilly et al. (2013): Bathtub model

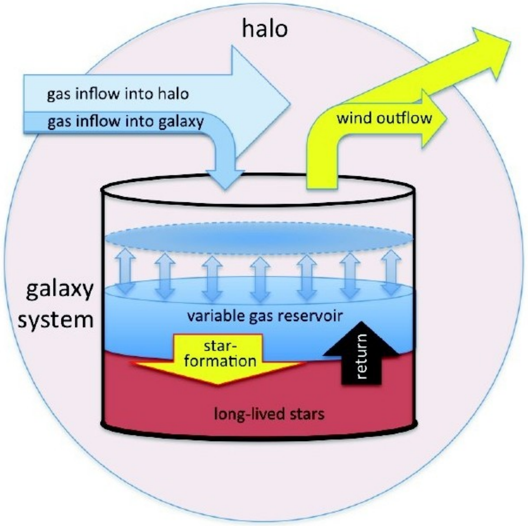

z<0.3 clusters: slow-then-rapid star-formation quenching

Roberts et al. (2019) & Maier, Ziegler, Haines & Smith (2019a)

Galaxies fly towards the center of the cluster:

- first, after passing R_{virial} (R_{200}), slow quenching (supply of pristine gas onto galaxy disk halted)
- then, above an ICM density threshold (derived from Chandra X-ray data at z<0.1), rapid quenching (quenched fraction increases faster) with cold gas affected by ram pressure

Slow-then-rapid quenching in clusters at z~0.2 revealed by higher gas metallicities inside R200 + comparing fractions of SF galaxies as function of clustercentric radius with simulations:
Quenching Timescales:

1-2 Gyr for slow-quenching using part of available gas reservoir,

~0.5-1Gyr for rapid quenching when ICM density higher (ram pressure > restoring pressure of the gas), when galaxies travel to denser inner regions of cluster

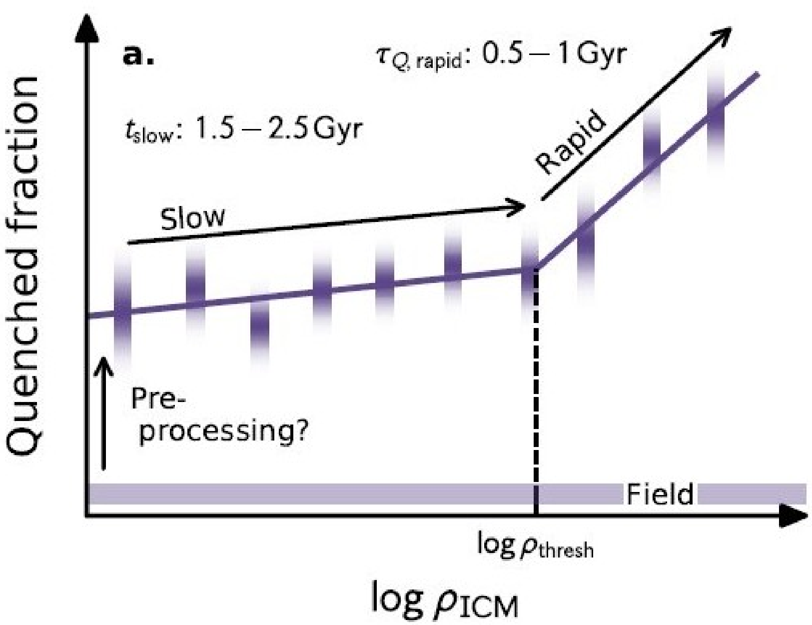

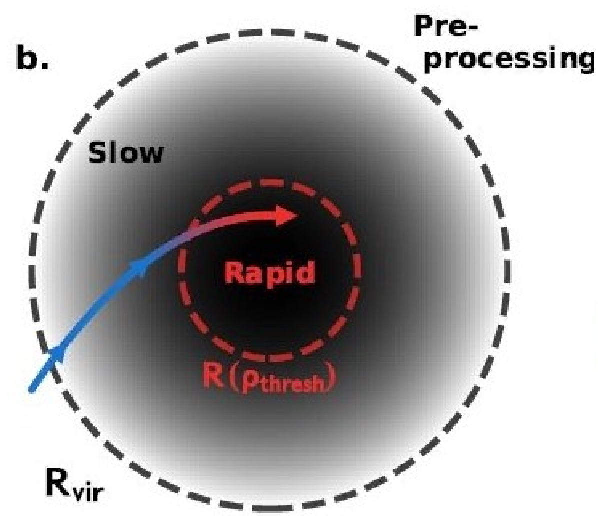

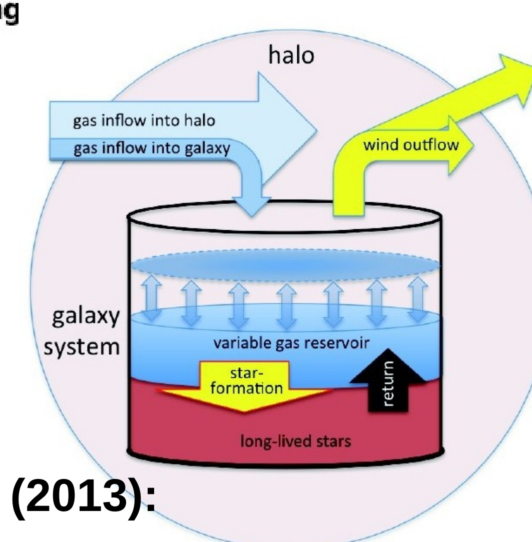

Lilly et al. (2013): Bathtub model

Do we see strangulation of cluster galaxies at z~1.5?

- cluster XMMXCSJ2215.9-1738 at z~1.5 (XMM2215 in the following)
- discovered in the XMM Cluster Survey (Stanford et al. 2006)

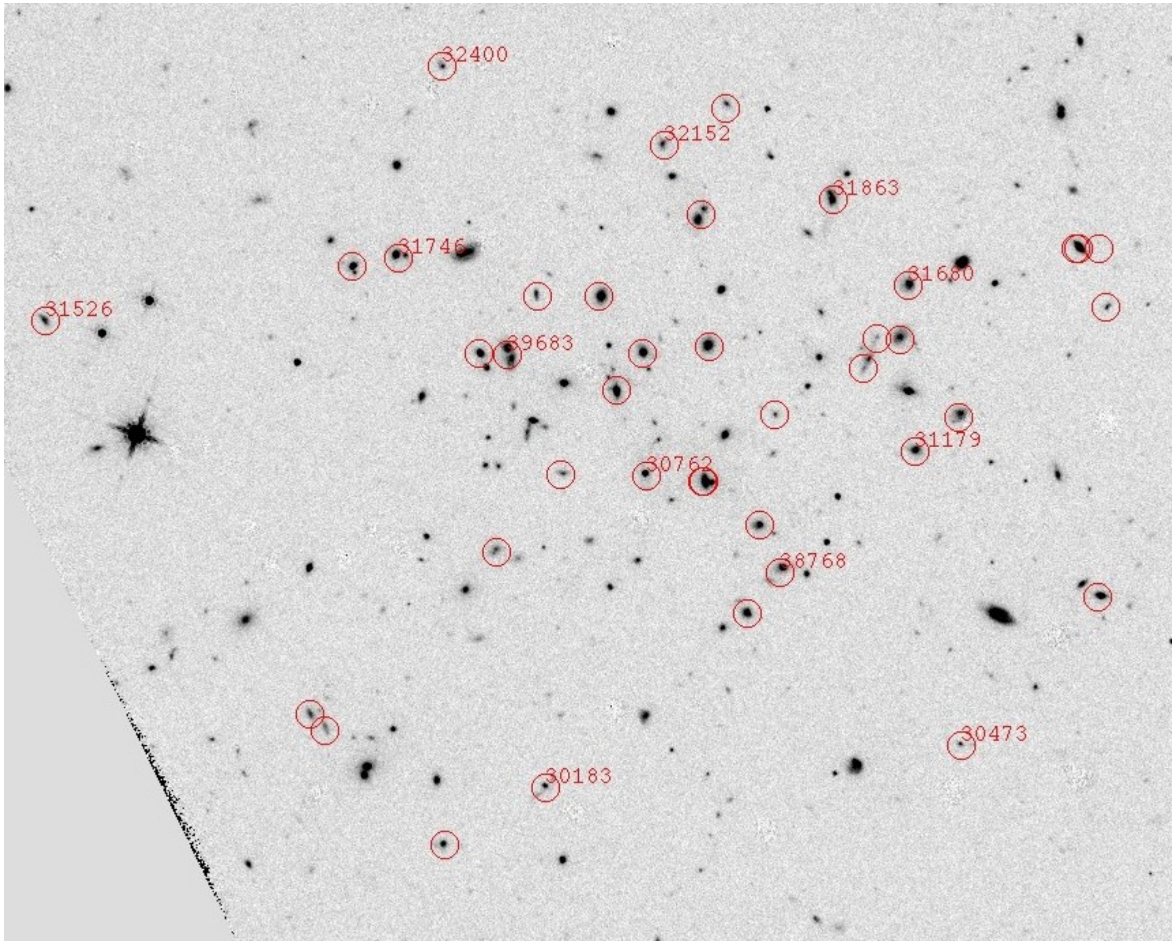

- M_{200}~ $6x10^{14}M_{sun}$
- extended emission from the hot gas: advanced evolutionary state
- a wealth of spectroscopic redshifts of XMM2215 cluster galaxies published (Hilton et al. 2009, 2010; Hayashi et al. 2011; Beifiori et al. 2017; Chan et al. 2018)

HST H-band image and spectroscopic cluster members at $R<0.5R_{200}$

Measured and derived quantities for 19 cluster galaxies

- KMOS spectroscopy of Hα and [NII] from the ESO archive covering about one virial radius R_{200} for 19 cluster galaxies
- 10 cluster galaxies with metallicity O/H measured from [NII]/Hα; 2 AGNs

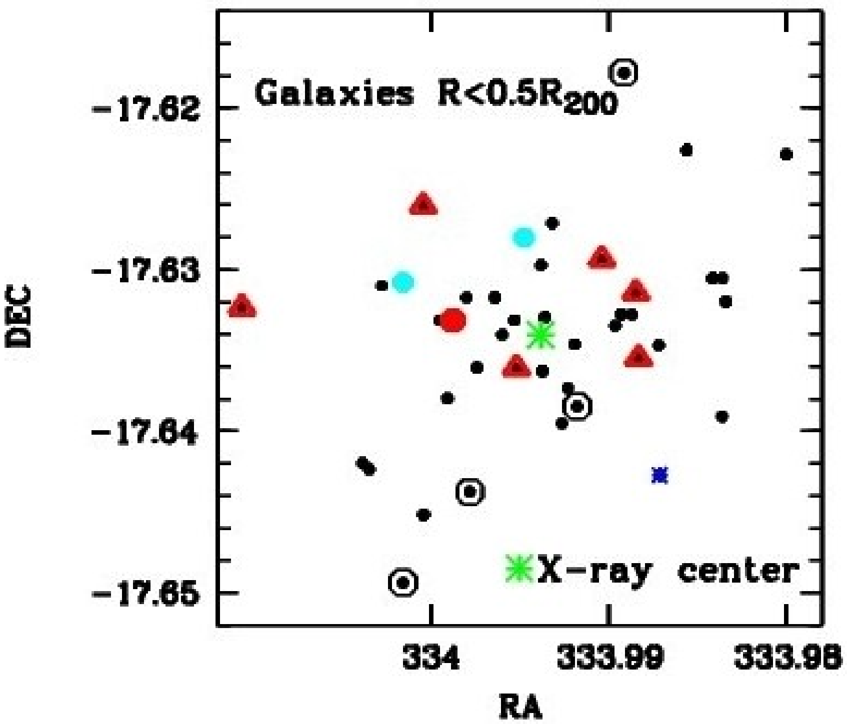

Maier et al. (2019b)

Id	spect. z	log[NII]/Hα	$\log(M/M_{\odot})$	O/H (PP04)	R/R_{200}
29284	1.461	-0.57 ± 0.08	$10.36^{-0.03}_{+0.03}$	8.57 ± 0.05	0.74
29609	1.459	[NII] on OH	$10.49^{-0.08}_{+0.11}$	*	0.44
30183	1.458	[NII] on OH	$10.18^{-0.04}_{+0.03}$	*	0.27
30473	1.446	< -0.71	$9.54^{-0.12}_{+0.11}$	< 8.50	0.28
30709	1.467	-0.73 ± 0.12	$10.56^{-0.04}_{+0.04}$	8.48 ± 0.07	0.71
30762	1.452	-0.42 ± 0.04	$10.45^{-0.08}_{+0.06}$	8.66 ± 0.02	0.06
31179	1.452	-0.56 ± 0.03	$10.40^{-0.03}_{+0.03}$	8.58 ± 0.02	0.14
31526	1.461	-0.50 ± 0.07	$10.24^{-0.05}_{+0.07}$	8.62 ± 0.04	0.41
31680	1.454	-0.44 ± 0.03	$10.67^{-0.04}_{+0.04}$	8.65 ± 0.02	0.15
31746	1.452	0.09 ± 0.08	*	AGN	0.21
31863	1.453	-0.38 ± 0.08	$10.97^{-0.06}_{+0.09}$	8.68 ± 0.04	0.15
32152	1.463	-0.04 ± 0.08	*	AGN	0.16
32400	1.454	-0.69 ± 0.11	$10.02^{-0.09}_{+0.08}$	8.51 ± 0.06	0.26
32650	1.460	[NII] on OH	$10.29^{-0.04}_{+0.04}$	*	0.95
33327	1.459	[NII] on OH	$10.59^{-0.04}_{+0.05}$	*	0.43
34305	1.455	-1.13 ± 0.19	$9.88^{-0.08}_{+0.09}$	8.26 ± 0.11	0.65
36109	1.469	< -0.77	$9.91^{-0.05}_{+0.08}$	< 8.46	0.56
38768	1.470	Hα on OH	$10.77^{-0.13}_{+0.13}$	*	0.12
39683	1.467	-0.20 ± 0.06	$11.39^{-0.13}_{+0.09}$	8.78 ± 0.03	0.12

Phase-space diagram for cluster XMM2215 at z~1.5

Cluster-centric radius vs. line-of-sight velocity relative to cluster redshift

- phase-space diagram (left panel) characterizes accretion state of cluster galaxies relatively free from effects due to the 2D projected positions with respect to the cluster center (right panel)
- phase-space diagram at $R<R_{200}$ using 58 cluster galaxies with spec-z

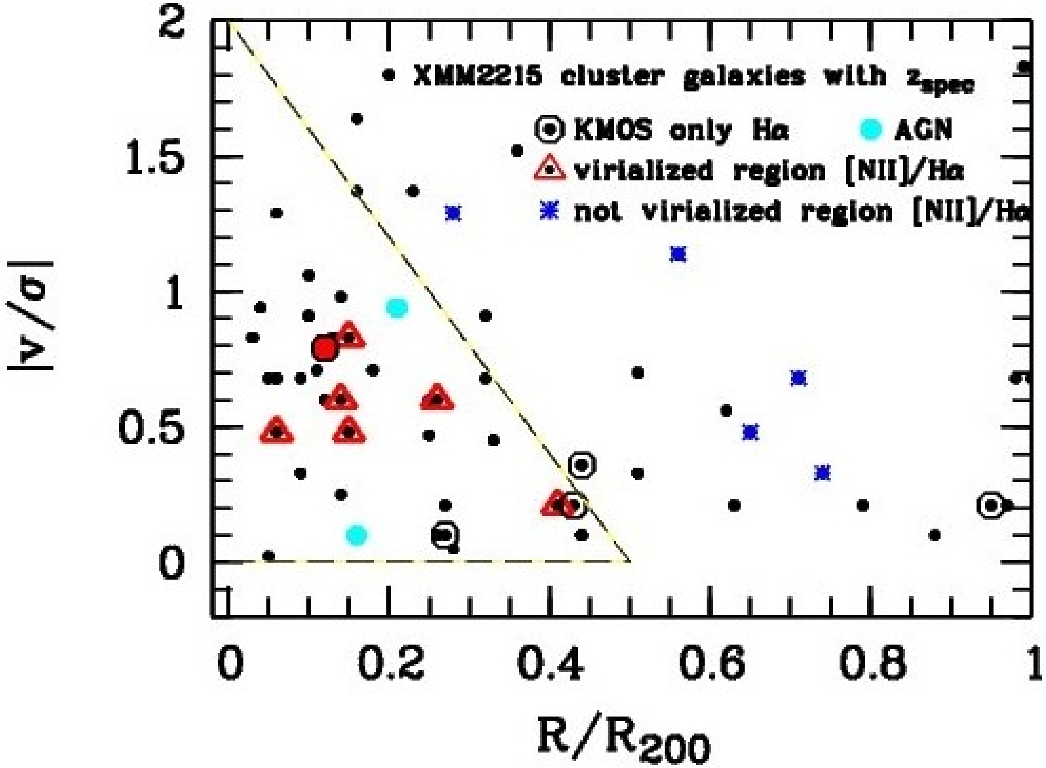

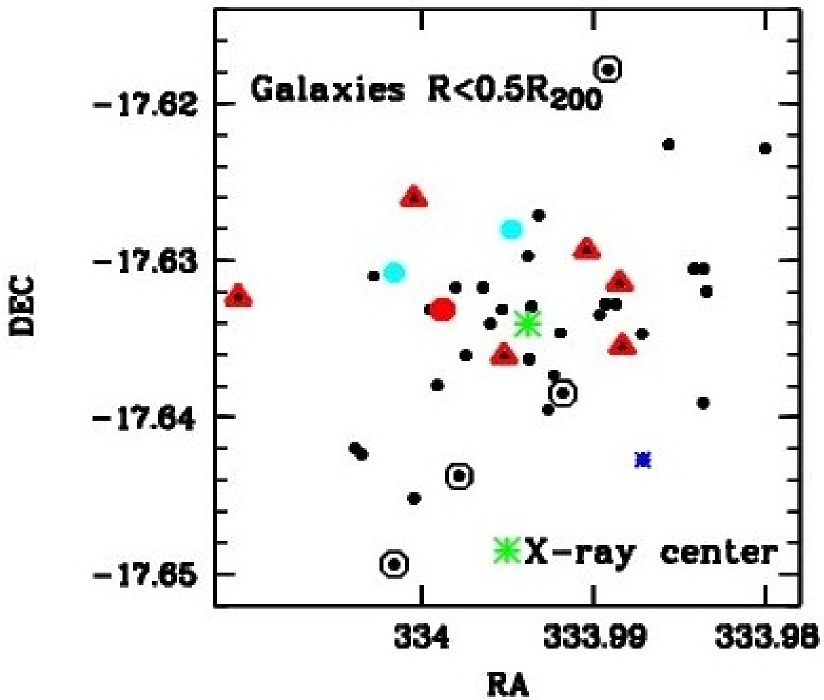

Phase-space diagram for cluster XMM2215 at z~1.5

- Dashed large triangle: virialized region derived by Rhee et al (2017) using cosmological hydrodynamic simulations of clusters
- galaxies with KMOS H-band spectroscopy: large symbols
- red filled circle: BCG (offset from X-ray centroid)
- infalling galaxies with KMOS spectroscopy: blue stars

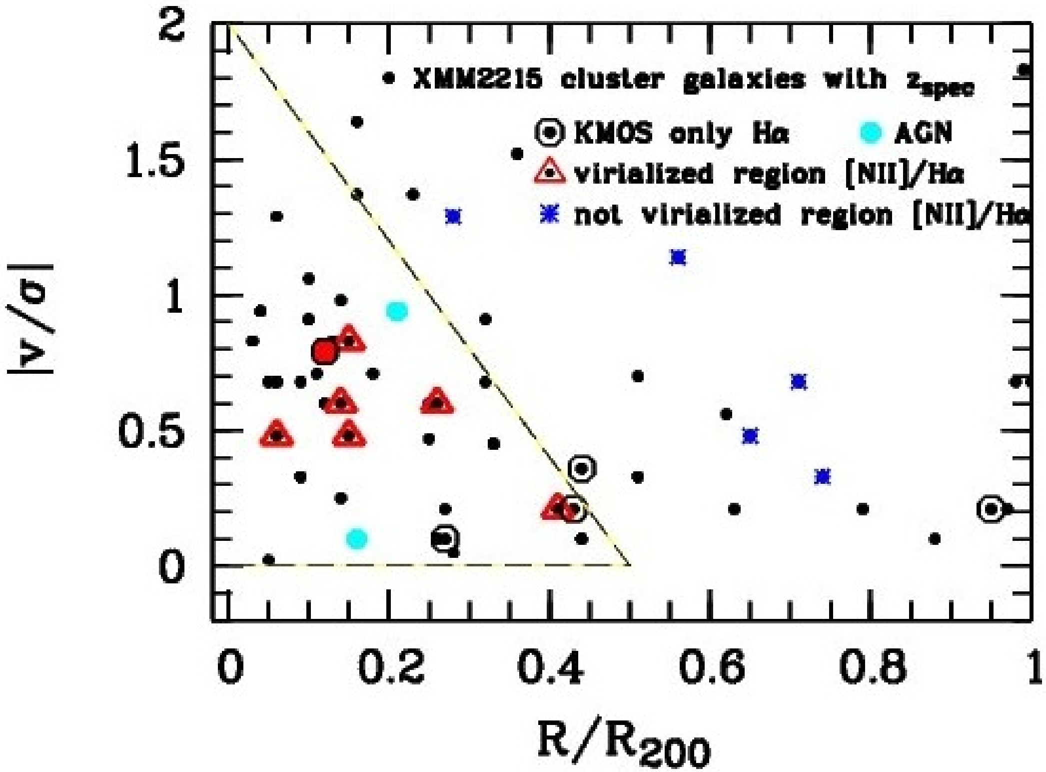

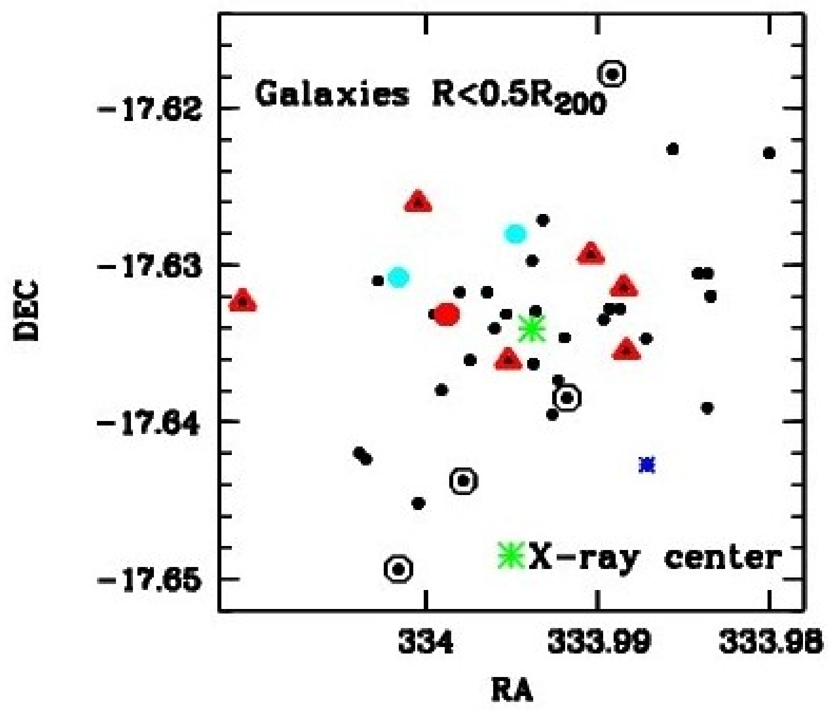

Mass-metallicity relation (MZR) & enhanced [NII]/Hα ratios

XMM2215 z~1.5 galaxies inside half R_{200} have higher metallicities by ~0.1dex (and higher [NII]/Hα ratios by ~0.2dex) than infalling galaxies and KMOS3D field galaxies at z~1.5,

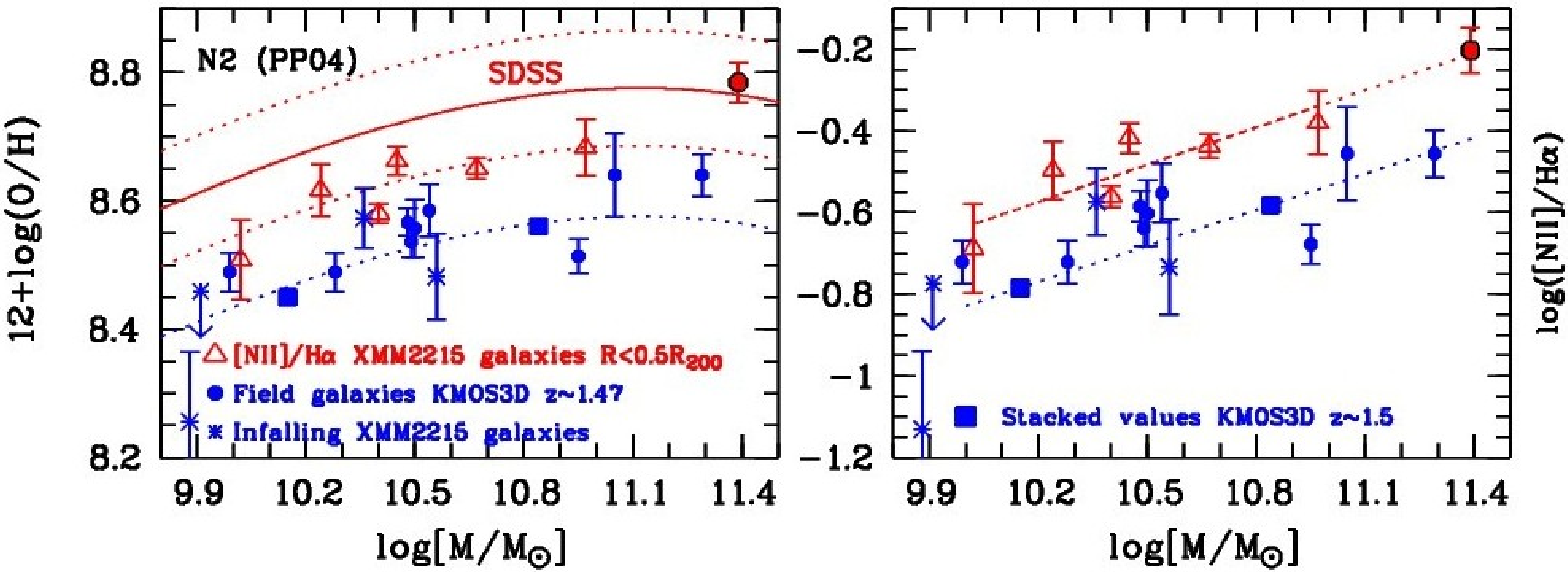

Mass-metallicity relation (MZR) & enhanced [NII]/Hα ratios

XMM2215 z~1.5 galaxies inside half R_{200} have higher metallicities by ~0.1dex (and higher [NII]/Hα ratios by ~0.2dex) than infalling galaxies and KMOS3D field galaxies at z~1.5, and slightly lower specific SFRs, but are still star-forming → slow quenching (strangulation)

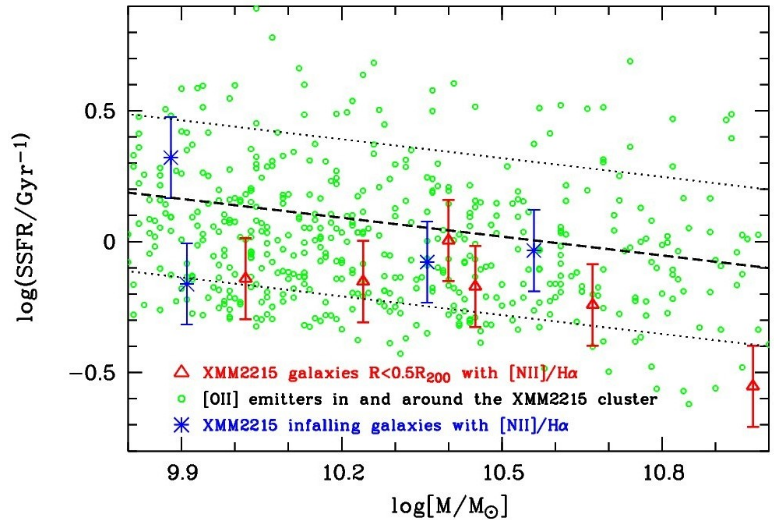

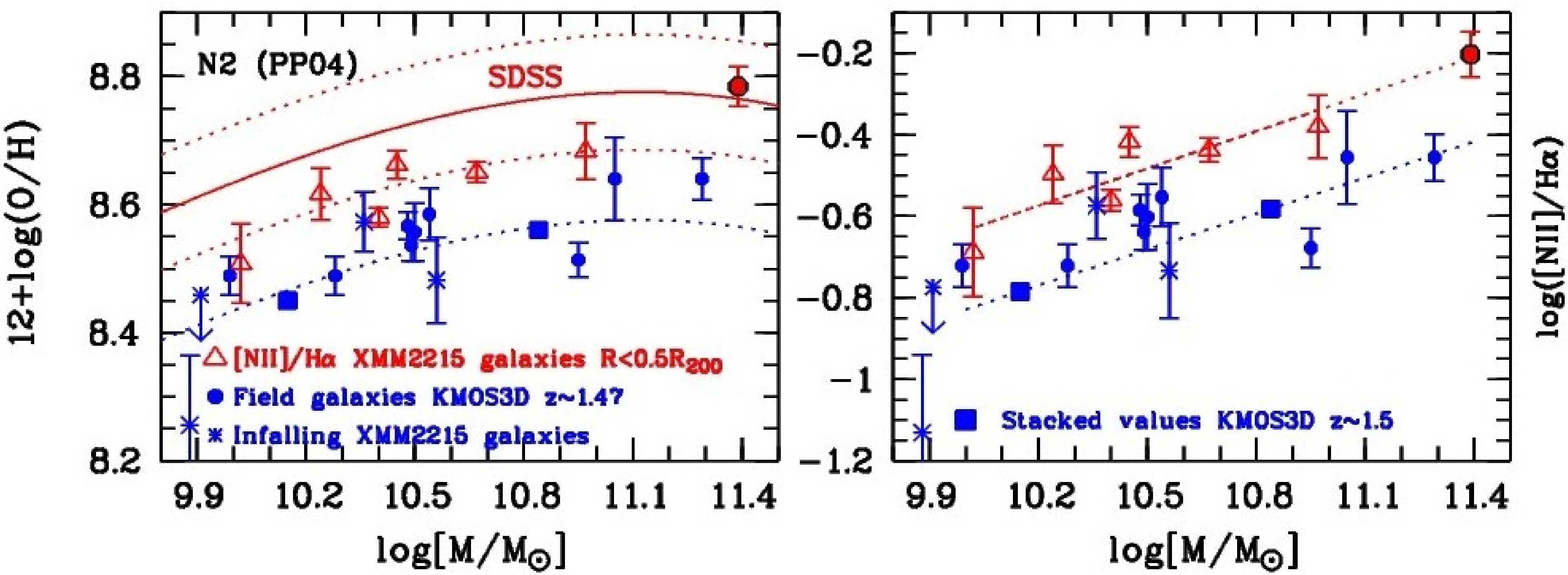

Maier et al. (2019b)

ALMA molecular gas

Hayashi et al. (2017, 2018): ALMA measurements of molecular gas in XMM2215

- CO emission line detection in some galaxies inside the triangle, some members not observed with ALMA: the main component of the stripped gas is the neutral gas, while the molecular gas (ALMA) is less affected by the ram pressure
- strangulated galaxies continue to form stars, using available cold gas in the disk which is not stripped

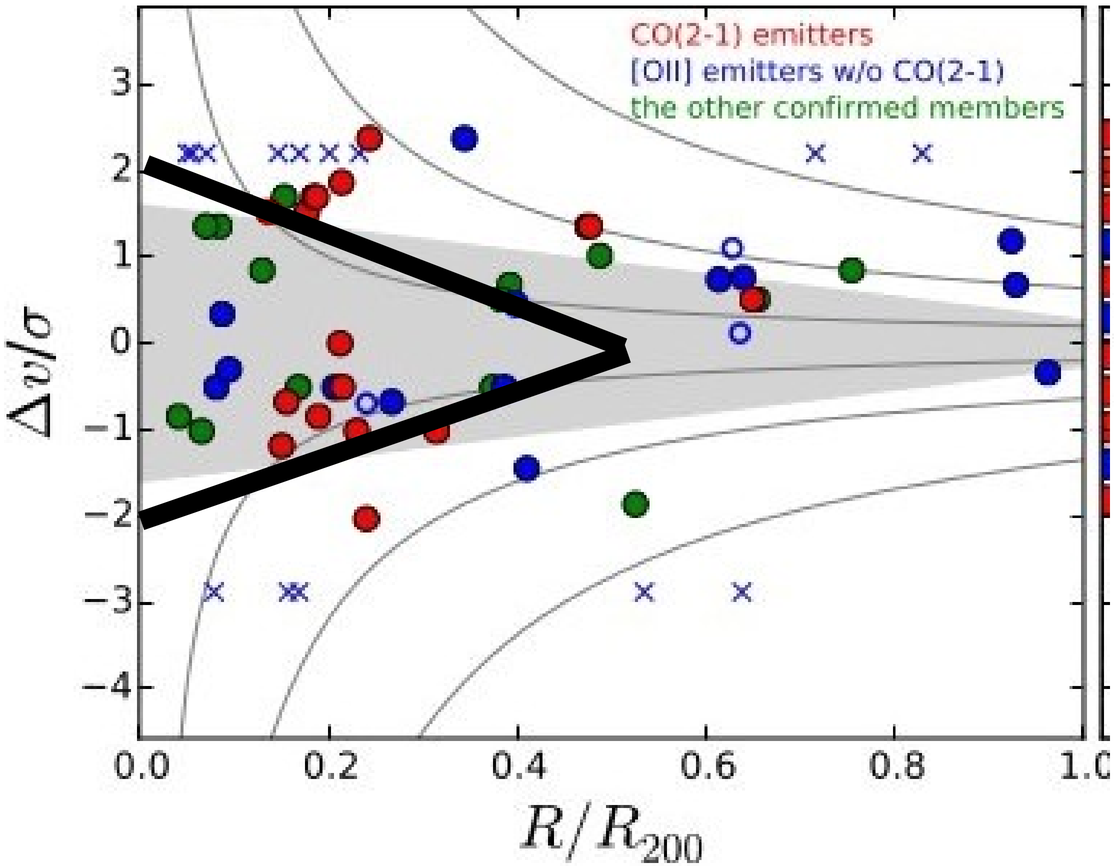

Hayashi et al. (2017)

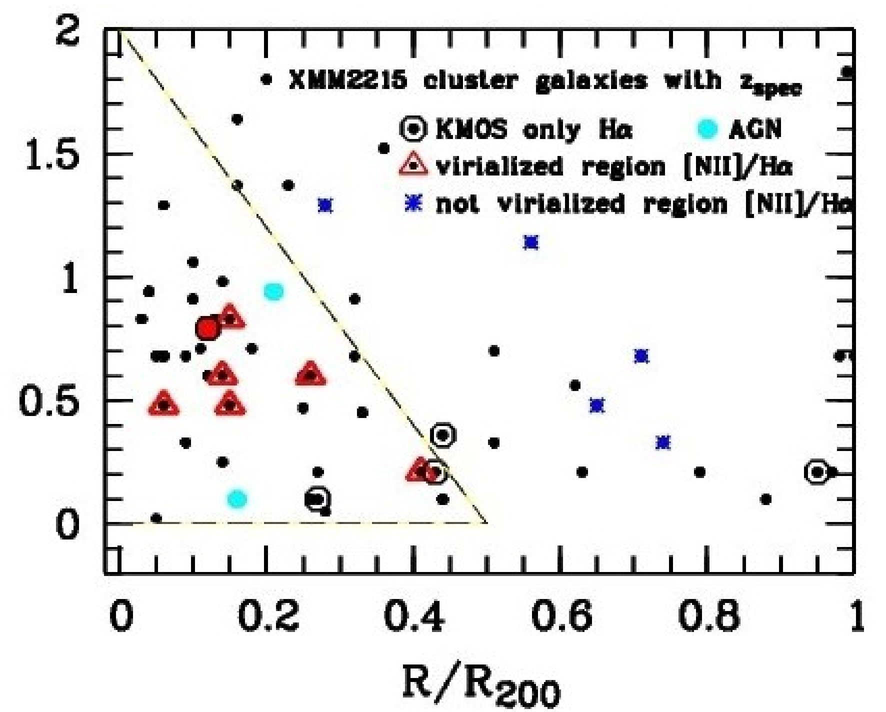

Maier et al. (2019b)

Side note: HSC-SSP protoclusters at z~1.5

- KMOS H-band observations of Hα for two protoclusters at z~1.5 selected from the HyperSuprimeCam-Subaru Strategic Program (Boehm et al. 2020), see E-Poster A5

A&A 633, A131 (2020)
https://doi.org/10.1051/0004-6361/201935527

Astronomy & Astrophysics

Kinematics of disk galaxies in (proto-)clusters at $z = 1.5^{\star}$

A. Böhm[1], B. L. Ziegler[1], J. M. Pérez-Martínez[1,2], T. Kodama[2], M. Hayashi[3], C. Maier[1], M. Verdugo[1], and Y. Koyama[4,5]

[1] Institute for Astronomy (IfA), University of Vienna, Türkenschanzstrasse 17, 1180 Vienna, Austria

Comparison with other cluster O/H studies at z~1.5

Chartab et al. (2021): MOSFIRE for [NII] and Hα of z~1.5 galaxies: higher O/Hs in overdense environments compared to field

- Agreement with the enhancement of 0.1dex in metallicities (compared to coeval field galaxies, KMOS3D) found by Maier et al. (2019b) inside half R_{200}

- Other studies (grey symbols): no enhancement in O/H in denser regions, but they assume that all cluster members have similar densities (both $R<0.5R_{200}$ & $R>0.5R_{200}$): this weakens any underlying environmental dependence of the MZR

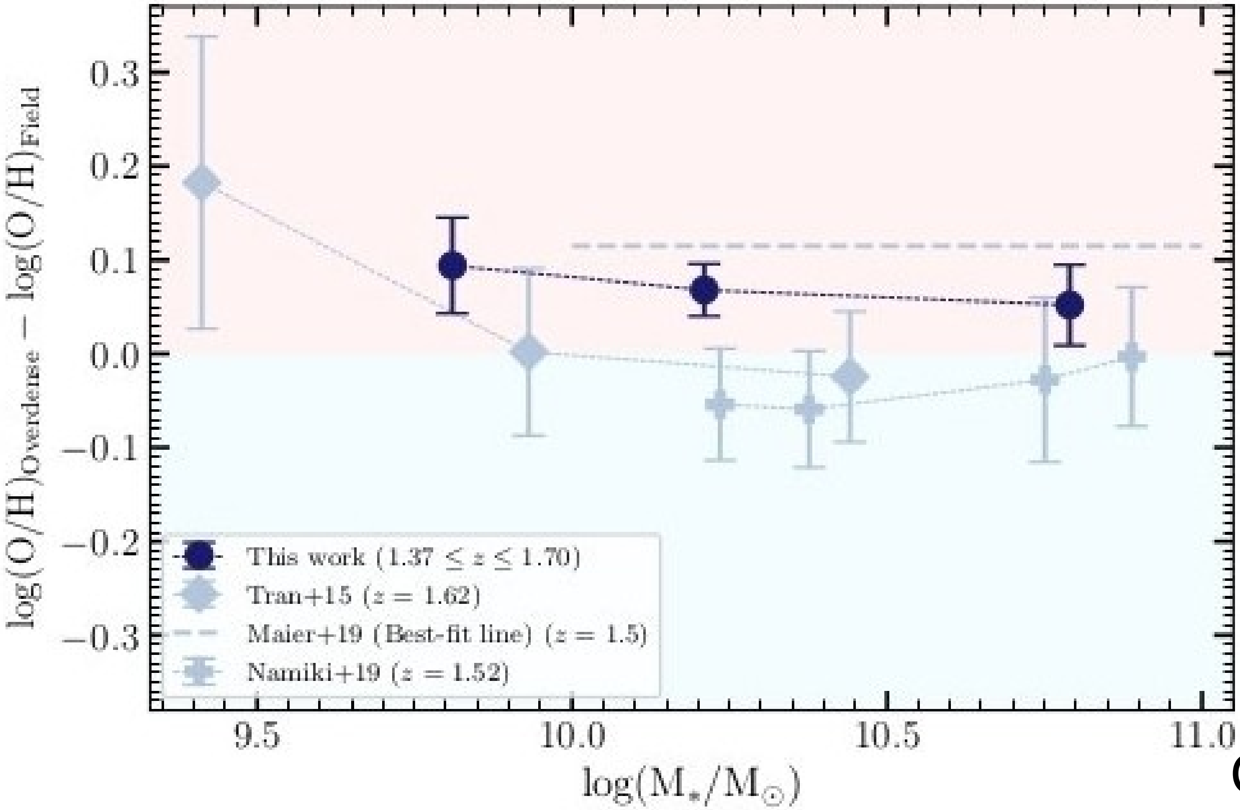

Chartab et al. (2021)

Conclusions

- KMOS H-band observations of [NII] and Hα for XMM2215 cluster galaxies at z~1.5, selected from the phase-space diagram to be at $R<R_{200}$: higher metallicities of galaxies inside half R_{200} compared to field galaxies (KMOS 3D) and infalling galaxies at similar redshifts

- evidence for slow quenching (strangulation) of cluster galaxies due to the stopping of the primeval gas inflow from the (neutral) gas reservoir which would otherwise dillute the ISM and maintain their ISM metallicities at field galaxies values

- cluster galaxies continue to form stars, albeit at slightly lower rates, using the available (molecular) cold gas in the disk which is not stripped